Int. J. Electrochem. Sci., 8 **(2013)** 7529 - 7541

International Journal of
ELECTROCHEMICAL
SCIENCE
www.electrochemsci.org

A Novel DNA Electrochemical Sensor Based on Grafting of *L*-Aspartic Acid and Cu^{2+} Ions on the Terminal of Molecule Beacons

Xia Wang[1,†], *Xuan Zhang*[1,†], *Cai Gao*[1], *Xiaolei Liao*[1], *Le Hang*[1], *Shulian Jiang*[2], *Feng Gao*[1], *Lizhang Huang*[2], *Qingxiang Wang*[1,*],

[1]Department of Chemistry and Environment Science, Zhangzhou Normal University, Zhangzhou 363000 P. R. China
[2]Zhangzhou Product Quality Supervision and Inspect ion Institute, Zhangzhou 363000, China
†These authors contributed equally to this work and should be considered co-first authors.
[*]E-mail: axiang236@126.com

Received: 11 April 2013 / *Accepted:* 15 May 2013 / *Published:* 1 June 2013

A novel electrochemical DNA biosensor based on *in-situ* labeling of *L*-Aspartic acid-copper ion (Asp-Cu^{2+}) complex on the terminal of molecule beacons (MBs) was constructed. The MB with bifunctional groups of 3'–SH and 5'–COOH was first anchored on a gold electrode surface through Au-S assembly chemistry, then *L*-Aspartic acid (Asp) was grafted with the 5'–COOH of MB via succinimide coupling, which was used as a platform molecule for the following coordination assembly of copper ions (Cu^{2+}). Therefore an electroactive MBs probe with the copper complex (Asp-Cu^{2+}) as a signal source was obtained. The hybridization between the loop sequence and the target DNA transferred the hairpin-like MBs to the linear form, and the electroactive moiety of Asp-Cu^{2+} was forced to leave away from the electrode surface, resulting in the reduction of the electrochemical response of the biosensor. The hybridization experiment results showed that the oxidation peak currents of developed biosensor attenuated linearly with the logarithmic values of the target DNA concentrations in the kinetic range from 1.0×10^{-15}~1.0×10^{-10} M. The detection limit was estimated to be 0.17 fM. Moreover, the biosensor showed excellent selectivity for discriminating the complementary sequences from the mismatched and noncomplementary sequences.

Keywords: Molecule beacon; *In-situ* labeling; *L*-Aspartic acid-copper complex; Electrochemical DNA sensor

1. INTRODUCTION

In the past two decades there has been a considerable growth of interest in sequence-specific DNA detection due to its significant potential in the application of clinical diagnosis, forensic and

environmental analysis, and food safety monitoring [1-3]. Based on the high specificity of base pairing principle of DNA, a variety of optical [4-6], acoustic [7, 8], and electronic [9, 10] ‘‘gene detection’’ approaches have been reported. Among these, a solution-phase optical approach termed molecular beacons (MBs) has attracted significant interest [11] because of its applicability to approach ranging from in vitro genotyping [12] to *in vivo* studies within single cells [13].

MBs are composed of a hairpin-like DNA stem–loop structure, with a fluorescent moiety and a fluorescence quencher attached to either terminus. In the absence of target, the molecular beacon is in the folded configuration in which its termini are held in close proximity and fluorescence emission is thus suppressed. Upon hybridization with a complementary target sequence, the stem–loop is converted into a rigid, linear double helix, removing the fluorophore from the quencher and greatly enhancing emission. Previous studies demonstrated that MBs can discriminate even single-base mismatches [14]. Whereas optical detection methods have historically dominated state-of-the-art real-time or near real-time genosensors [1, 15, 16], the application of electrochemical methods to the sensing of biologically related species may provide very significant advantages, including speediness, sensitivity, and low cost power requirements [17, 18].

Fan et al. [19] first reported a strategy for the reagentless transduction of DNA hybridization into a readily detectable electrochemical signal by means of a conformational change analogous to the optical molecular beacon approach, in which an electroactive ferrocene-tagged DNA stem–loop structure was applied as an electroactive MB. Through hybridization, a great conformational change in this surface-confined DNA structure significantly alters the electron-transfer tunneling distance between the electrode and the redox-active label, resulting in variation in electron transfer efficiency. As compared with the existing optical approaches, the electrochemical MB biosensor can detect femtomoles of target DNA without employing cumbersome and expensive optics, light sources, or photodetectors, offering the great promise of convenient, reusable detection of picomolar DNA.

However, the most used electroactive MBs are obtained through homogeneous solution synthesis, including the procedures of bioconjugation (i. e., the coupling between succinimide ester of ferrocene carboxylic acid and 5’ modified MB [20]), separation and purification, and so on, which significantly increased the cost and the complexity of this type of biosensors. In order to circumvent this problem, a new strategy based on *in-suit* labelling an electrochemical metal complex on the free terminal of immobilized MBs was constructed in this work. The main concept was illustrated in Figure 1. Firstly, MBs with bifunctional groups of 3’–SH and 5’–COOH were anchored on a gold electrode surface through Au-S assembly chemistry, then the 5’–COOH was transferred to succinimide ester with the aid of 1-(3-Dimethylaminopropyl)-3-ethylcarbodiimide hydrochloride (EDC), *N*-Hydroxysulfosuccinimide sodium salt (sulfo-NHS), which was further grafted with a platform molecule of *L*-Aspartic acid (Asp). Lastly, based on the strong coordination between the grafted Asp and copper ion (Cu^{2+}), the electroactive element (Cu^{2+}) was labeled on the MB, thus an electrochemical MB biosensor was constructed. Before hybridization with target DNA, the stem-loop conformation of MBs forces the redox reporter (Asp-Cu^{2+}) into proximity with the electrode, ensuring efficient electron transfer. However when the loop was hybridized to a complementary DNA, the MBs was changed to a relatively rigid, double–stranded conformation, by which the electrons transfer was significantly reduced. The experiment result showed that the oxidation peak currents of developed

biosensor attenuated linearly with the logarithmic values of the target DNA concentrations in the kinetic range from 1.0×10^{-15}~1.0×10^{-10} M. The detection limit was estimated to be 0.17 fM.

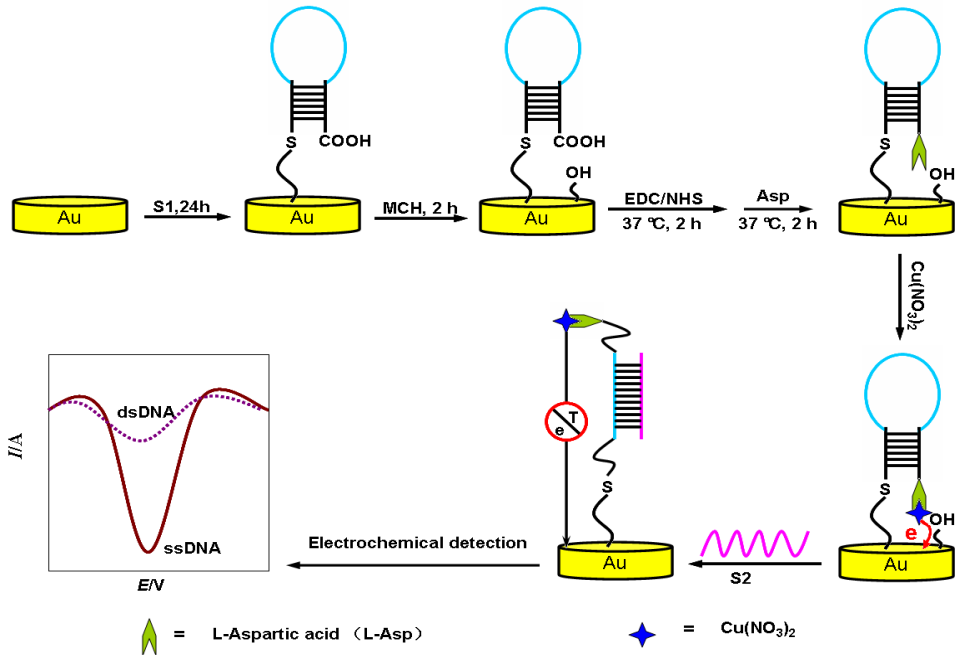

Figure 1. The schematic of electrochemical DNA sensor based on *in-situ* grafting of electroactive *L*-Aspartic acid-Cu^{2+} complex on the free terminal of the molecule beacons

2. EXPERIMENTAL PART

2.1. Reagents and Apparatus

Electrochemical experiments including cyclic voltammetry (CV), electrochemical impendence spectra (EIS) and differential pulse voltammetry (DPV) were measured on a CHI 650D electrochemical analyzer (Shanghai CH Instrument, China). A conventional three-electrode system was used with a bare or modified Au disk working electrode, a platinum wire auxiliary electrode and an Ag/AgCl(3 M KCl) reference electrode. The geometric area of the working electrode is 3.1×10^{-2} cm^2 obtained from the diameter of 2 mm.

Ethylenediaminetetraacetic acid (EDTA) was purchased from Xilong Chemical Co., Ltd (China); 1-(3-Dimethylaminopropyl)-3-ethylcarbodiimide hydrochloride (EDC), *N*-Hydroxysulfosuccinimide sodium salt (sulfo-NHS) and Tris (2-carboxyethyl) phosphine hydrochloride (TCEP) and 6-Hydroxy-1-hexanethiol (MCH) were purchased from Sigma-Aldrich (China); Tris (hydroxymethyl) aminomethane (Tris) was purchased from Shanghai Jingchun Reagent Co., Ltd (China). *L*-Aspartic acid and $Cu(NO_3)_2$ were provided by Aladdin Reagent Company (China). All the other chemicals were of analytical reagent grades and were obtained commercially. Doubly distilled water (DDW) was used throughout this experiment.

All the oligonucleotides were synthesized by Shanghai Sangon Bio-engineering Ltd. Company (China) and their base sequences were as follows:

MB probe (S1): 5'-COOH-$(CH_2)_6$-GCGAGTCTTTGGGACCACTGTCGCTCGC- $(CH_2)_6$-SH-3';

Complementary Sequence (S2):5'-CGACAGTGGTCCCAAAGA-3';

Single-base mismatched sequence (S3):5'-CGACAGTGGTCCCAACGA-3';

Three-base mismatched sequence (S4):5'-CGACAATGGCCCCAACGA-3';

Non-complementary sequence (S5):5'-GCATCGAGCGAGCTCGTA-3'.

DNA immobilization buffer (IB, pH 8.0) was prepared by mixing 0.10 M NaCl, 0.10 M $MgCl_2$, 10.0 mM TCEP and 25.0 mM Tris-HCl. The hybridization buffer was 10.0 mM PBS (pH 7.0) with 25.0 mM NaCl. The electrolyte for the electrochemical hybridization detection was 0.10 M H_3BO_3 (pH 8.0) containing 0.1 M KCl and 2.5% (*V*/*V*) ethanol.

2.2 Immobilization of S1 on gold electrode surface

Prior to use, the bare Au electrode was polished to a mirror-like surface with 0.5 μm, 0.3 μm and 0.05 μm α-Al_2O_3, respectively, and rinsed ultrasonically with DDW, absolute ethanol and DDW, in turn. Then, the electrode was immersed in Piranha solution ($V(H_2SO_4):V(H_2O_2)$=7:3) for 10 min, which was followed by repeatedly scanned in 0.5 M H_2SO_4 from +1.6 V to -0.2 V for 50 cycles to obtain the steady curve. Afterwards, the electrode was rinsed with DDW and dried under a stream of nitrogen. Then the pre-treated electrode was immersed into IB containing 1.0×10^{-7} M S1 for 24 h to achieve probe DNA modified electrode through Au-S chemistry. After rinsing, the modified electrode was treated with 1.0 mM MCH solution for 2 h to mask the unmodified Au sites. Thus, the DNA biosensor (MCH/S1/Au) was prepared.

2.3 Grafting of Asp on the terminal of probe DNA

The grafting of Asp on the terminal of immobilized MBs was achieved by a typical amide condensation [21]: in brief, MCH/S1/Au was first immersed into 1 mL 5.0×10^{-2} M PBS containing 1.0 mM EDC and 5.0 mM sulfo-NHS for 2 h at 37 ℃ to pre-activate the carboxylic groups on 5' end of S1. After rinsing with PBS, the electrode was immersed in 1.0 mM Asp for another 2 h at 37 ℃. After being washed with PBS to remove the unbound Asp, the Asp grafted electrode was obtained, which was denoted as Asp/MCH/S1/Au.

2.4 Coordination assembly of Cu^{2+} ions

The coordination process of Cu^{2+} ion with the grafted Asp was performed by incubating Asp/MCH/S1/Au in 5 mM $Cu(NO_3)_2$ for 30 min, and then eluting the nonspecifically absorbed Cu^{2+} ions with the mixing solution of 25 mM NaCl and 10 mM PBS (pH 7.0) for 40 min, thus the Cu^{2+} ion labeled MB biosensor was prepared, which was denoted by Cu^{2+}-Asp/MCH/S1/Au.

2.5 Hybridization and electrochemical detection of the biosensor

The hybridization reaction was performed by immersing Cu^{2+}-Asp/MCH/S1/Au into 200 μL hybridization buffer containing different targets for 40 min at 37 ℃, and then rinsed with DDW to remove the unhybridized DNA. The hybridized electrode was denoted as Cu^{2+}-Asp/MCH/S2-S1/Au, Cu^{2+}-Asp/MCH/S3-S1/Au, Cu^{2+}-Asp/MCH/S4-S1/Au or Cu^{2+}-Asp/MCH/S5-S1/Au.

Electrochemical characterization on the fabrication process of the biosensor was carried out in 1.0 mM $[Fe(CN)_6]^{3-/4-}$ solution containing 0.1 M KCl via CV and EIS. The scan range for CV was between -0.2 and +0.6 V and the scan rate was 100 mV/s. The EIS was collected at a potential of +0.207 V in the frequency range of 10^5~1 Hz with the voltage amplitude of 5 mV.

The hybridization detection of the biosensor was carried out with CV and DPV in 0.10 M H_3BO_3 (pH 8.0) containing 0.1 M KCl and 2.5% (*V/V)* ethanol. The scan range for CV was between -0.2 V to +0.6 V. The DPV was recorded within the potential range from -0.2 V to +0.6V with a pulse amplitude 0.05 V, pulse width 0.05 s and pulse period 0.2 s.

3. RESULTS AND DISCUSSION

3.1 Electrochemical characterization on the immobilization of MB and the grafting of the Asp

In this work, in order to obtain a novel electroactive MBs, the platform molecule of Asp and the electroactive unit of Cu^{2+} ions were layer-by-layer assembled on the carboxylic group modified MB through covalent coupling and coordination, respectively. The assembly process was characterized by CV and EIS methods using $[Fe(CN)_6]^{3-/4-}$ as the electrochemical probe, and the results were showed in Figure 2. From the CV results (Figure 2A), it could be seen that the redox peaks on MB (S1) modified Au electrode (curve b) was much smaller than those on bare Au electrode (curve a) due to the electrostatic repulsion between the negatively charged phosphate backbone and $[Fe(CN)_6]^{3-/4-}$ ions, which suggested that the MB had been immobilized on the basal electrode surface. When MCH sealed the rest sites of the electrode surface, the redox peaks of $[Fe(CN)_6]^{3-/4-}$ were further reduced (curve c). By this step, the immobilized MB on electrode surface could maintain the better orientation for hybridization and the nonspecific absorption of the other substances on the electrode surface could be well prevented [22]. Further, when the platform molecules of Asp were covalently grafted on the free 5' terminal of MB through the amide condensation with the aid of EDC/sulfo-NHS, the electrochemical response of $[Fe(CN)_6]^{3-/4-}$ on the modified electrode was further suppressed (curve d). This was likely caused by the increase of the steric hindrance on electrode surface and the repulsion of the negatively charged Asp moiety toward the $[Fe(CN)_6]^{3-/4-}$.

Electrochemical impedance spectroscopy (EIS) is a method of monitoring the impedance of the surface during the process of frequency variation, which offers various properties of the interface between the electrode and the solution, including the electrode impedance, the capacity of the electric double layer, and the surface electron transfer resistance (R_{ct}) [23]. The fabrication process of the biosensor was also characterized by EIS, and the results are shown in Figure 2B. The Nyquist plot for the bare Au electrode exhibited a semicircle portion at the higher frequencies relating to the electron

transfer-limited process and a linear part at the lower frequencies corresponding to the diffusion process (curve a). From the diameter of the semicircle, the value of R_{ct} was estimated to be 500 Ω. After modification with MB, the value of R_{ct} increased to 4250 Ω (curve b). When MCH was further assembled, the value of R_{ct} was changed to 4750 Ω (curve c), also suggesting that the MCH molecules had occupied the unmodified sites. On the Asp grafted electrode surface, the R_{ct} was further increased to about 10000 Ω (curve d), indicating that the kinetic resistance of $[Fe(CN)_6]^{3-/4-}$ on the electrode surface was further enhanced by the grafted Asp molecule. All these results clearly suggested that the MB and the terminal platform molecules had been successfully modified on the electrode surface by the layer by layer assembly.

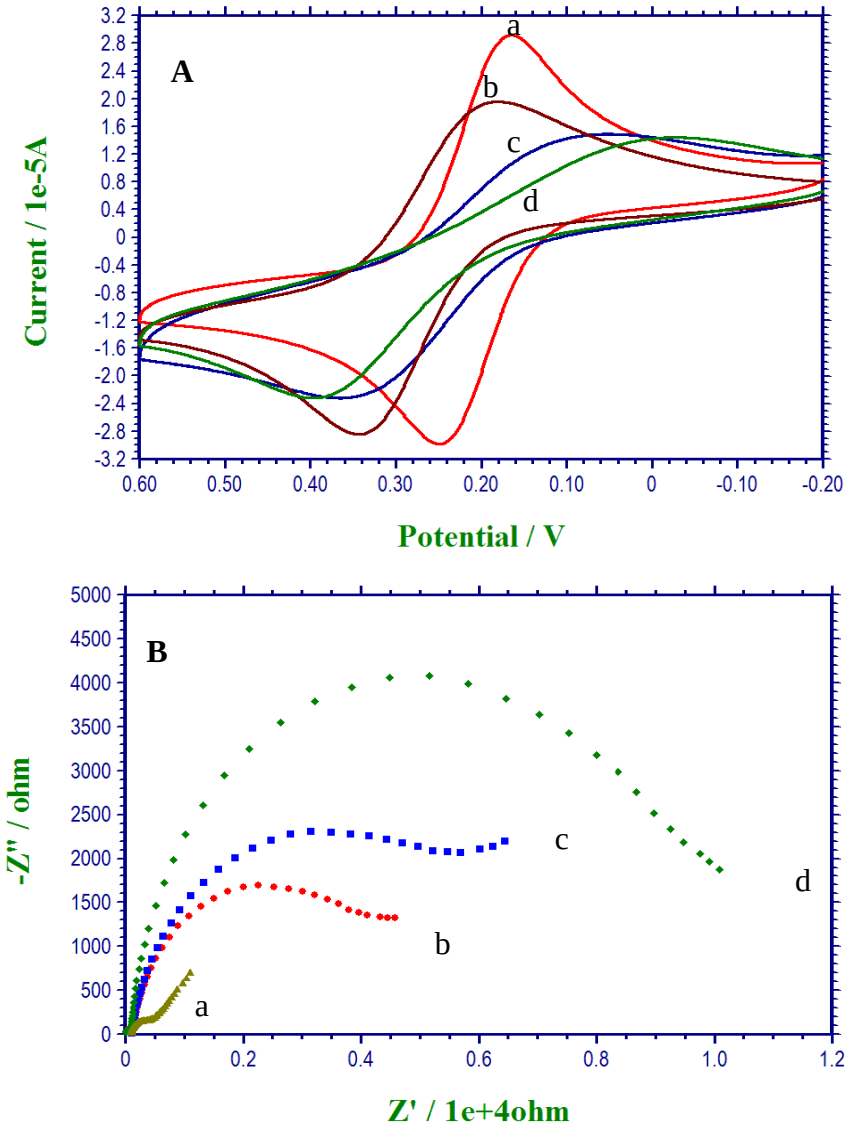

Figure 2. Cyclic voltammograms (A) and electrochemical impedance spectroscopy (B) of 1.0 mM $[Fe(CN)_6]^{3-/4-}$ with 0.1 M KCl recorded on bare Au (a), S1/Au (b), MCH/S1/Au (c), Asp/MCH/S1/Au (d)

3.2 Coordination assembly of Cu^{2+} on Asp/MCH/S1/Au and its electrochemical behaviors

Cu^{2+} is a kind of inexpensive and safe transition metal ion that has excellent electrochemical property [24, 25]. In addition, it has strong coordination ability with many amino acids such as Asp [26], glycine [27] and *L*-threonine [28]. Based on these features, the Cu^{2+} ion was chose as the electroactive element to construct the electrochemical MB probe. Figure 3 shows the CVs of Asp/MCH/S1/Au before (curve a) and after (curve b) incubating in Cu^{2+} ions solution. Obviously, there were not any Faradic electrochemical response for Asp/MCH/S1/Au electrode in supporting electrolyte (0.1 M H_3BO_3 containing 0.1 M KCl and 2.5%(*V*/*V*) ethanol, pH 8.0), suggesting that all the components of Asp/MCH/S1/Au was electroinactive under the testing solution. However, after the Asp/MCH/S1/Au was accumulated with Cu^{2+}, a pair of obvious redox peaks were observed at +0.376 V and +0.047 V, which was well consistent with the electrochemical characteristic of the Cu^{2+}/Cu^{+} redox couple [28], suggesting that the electroactive Cu^{2+} had been successfully anchored on the electrode surface through the developed approach.

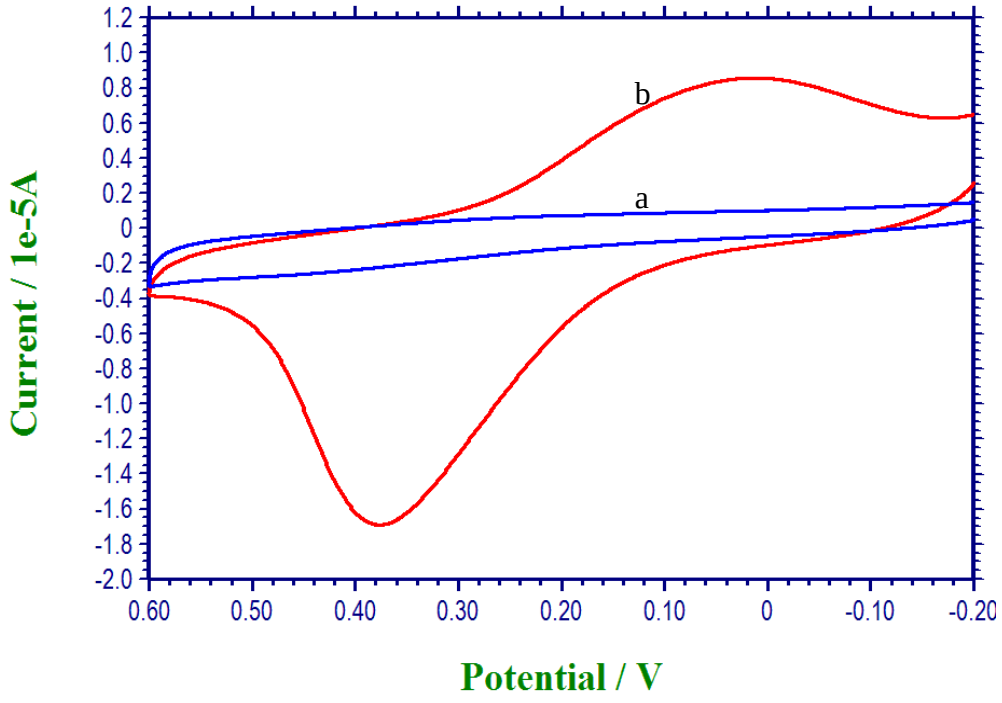

Figure 3. Cyclic voltammograms of Asp/MCH/S1/Au (a) and Cu^{2+}-Asp/MCH/S1/Au (b) in supporting electrolyte (0.1 M H_3BO_3 containing 0.1 M KCl and 2.5% (*V*/*V*) ethanol, pH 8.0), scan rate: 100 mV/s.

The scan rate assay showed that both the oxidation and reduction peaks were changed with the variation of the scan rate (Figure 4), and both the oxidation peak currents (I_{pa}) and reduction peak currents (I_{pc}) presented good linear relationships with the scan rate (v): $I_{pa}(10^{-6}A)$=-0.912-0.044v(mV/s), r=0.998; $I_{pc}(10^{-6}A)$=0.744+0.011v(mV/s), r=0.982, demonstrating that the electrochemistry was controlled by an adsorption process, which was in agreement with the conclusion that the Cu^{2+} had been assembled on the electrode surface.

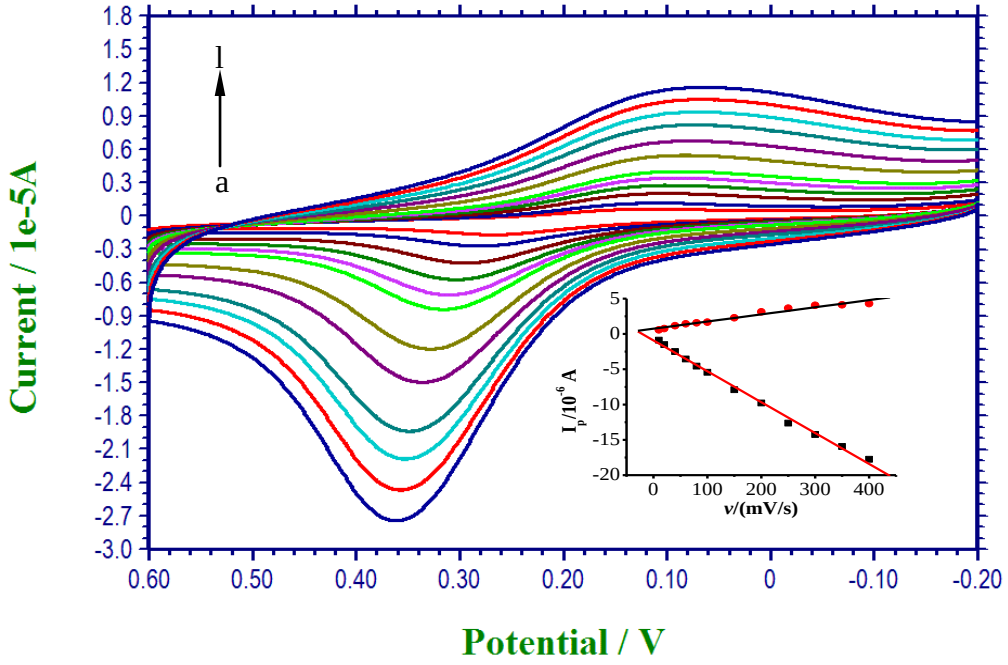

Figure 4. Cyclic voltammograms of Cu^{2+}-Asp/MCH/S1/Au (b) in supporting electrolyte with different scan rate (a~l: 10, 20, 40, 60, 80, 100, 150, 200, 250, 300, 350, 400 mV/s); inset: the relationship of peak currents (I_p) with the scan rate (v).

3.3 Optimization of the experimental conditions

In order to obtain the most sensitive electrochemical response of the biosensor, the fabrication and detection conditions of the biosensor were optimized. Firstly, it has been reported that the presence of certain amount of ethanol in the test electrolyte can effectively improve the stability and electrochemical sensitivity of the copper complex [29], therefore in this work, the influence of the ethanol on the electrochemical behaviors of the biosensor was also investigated, and it was found that when the content of ethanol was at 2.5% (*V*/*V*), Cu^{2+}-Asp/MCH/S1/Au revealed the largest electrochemical signal, therefore in this work the solution of 0.1 M H_3BO_3 (pH 8.0) containing 0.1 M KCl and 2.5% (*V*/*V*) ethanol was chose as the supporting electrolyte.

Secondly, the effect of coordination assembly time of Asp/MCH/S1/Au with Cu^{2+} on the electrochemical signal of the biosensor was investigated. Fig. 5B shows the relationship between the oxidation peak currents and the accumulation time. It was observed that with the increase of the accumulation time, the electrochemical signal corresponding to the Cu^{2+} increased, and when the time reached to the 40 min, the peak currents tended to be constant, suggesting the coordination saturation between Asp and Cu^{2+} on the electrode surface. In addition, with the consideration of the nonspecific absorption of Cu^{2+} on the electrode surface (*i. e.*, the electrostatic interaction of Cu^{2+} with the phosphate background of MB), the elution experiment was investigated using 25 mM NaCl mixing with 10 mM PBS (pH 7.0) under stirring as the eluting solution, and the results showed that the with the prolonging of elution time, the peak currents decreased rapidly in the first stage. When the time

exceeded 40 min, the peak currents became stable (Fig. 5C), suggesting the loosely absorbed Cu^{2+} had been removed from the electrode surface.

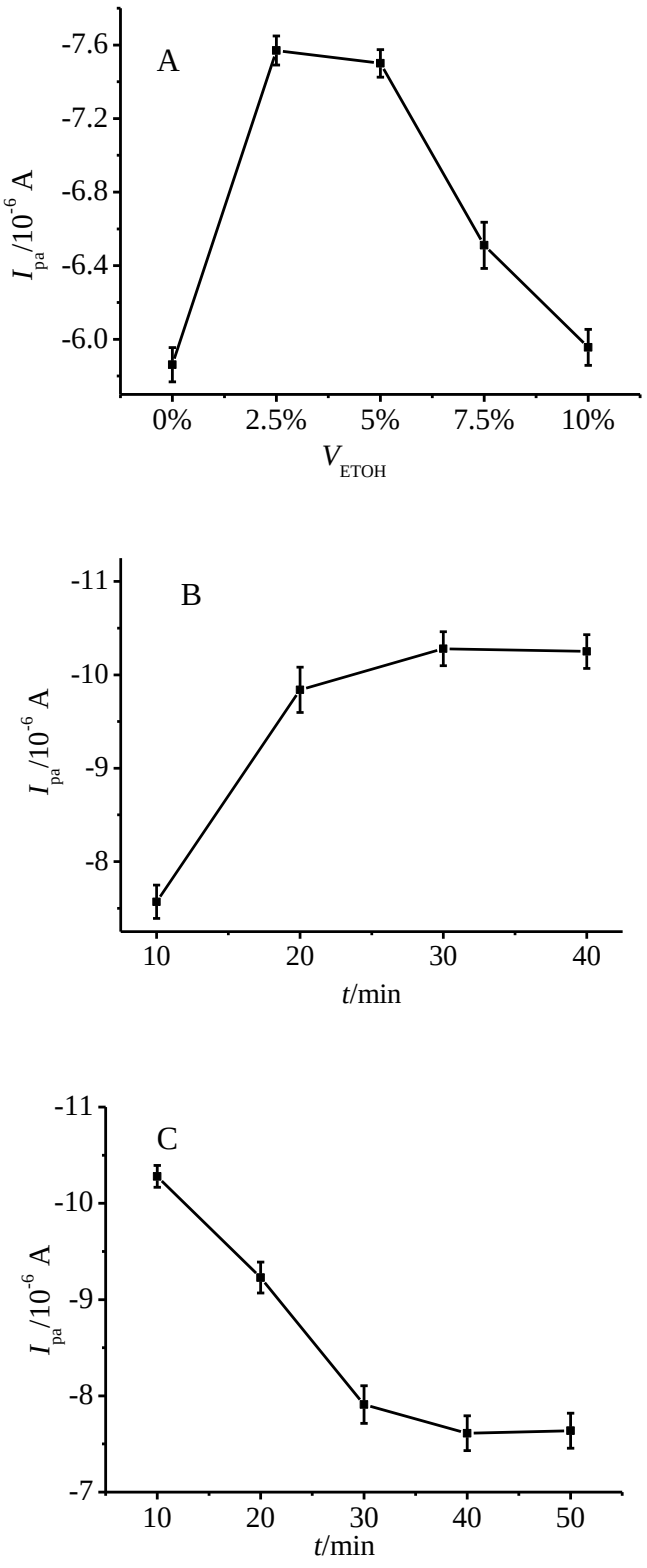

Figure 5. The relationship of oxidation peak currents of Cu^{2+}-Asp/MCH/S1/Au with content (*V/V*) of ethanol in the test electrolyte (A), with the accumulation time of Cu^{2+} (B), or with the elution time (C)

3.4 Analytical performances of the biosensor

The analytical performance of the developed biosensor was evaluated by hybridization selectivity and sensitivity experiments. Fig. 6 shows the DPVs of Cu^{2+}-Asp/MCH/S1/Au in supporting electrolyte before (curve a), and after hybridization with complementary sequence of S2 (curve e), one-base mismatched sequence of S3 (curve d), three-base mismatched sequence of S4 (curve c) and non-complementary sequence of S5 (curve b), respectively. It was observed that a large oxidation peak occurred at +0.18 V, which can be ascribing to the reason that the grafted electroactive unit of Asp-Cu^{2+} on the free terminal of unhybridized MB was closed to the electrode surface, and can communicate electron with the electrode easily [19].

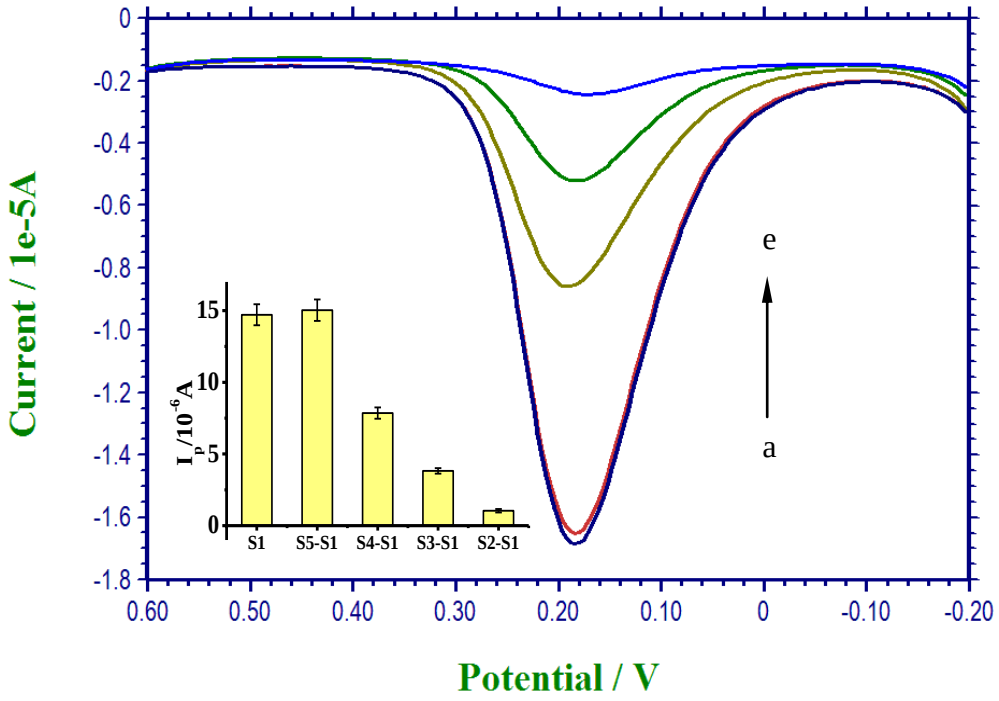

Figure 6. DPVs of Cu^{2+}-Asp/MCH/S1/Au before (curve a), and after hybridization with complementary sequence of S2 (curve e), one-base mismatched sequence of S3 (curve d), three-base mismatched sequence of S4 (curve c) and non-complementary sequence of S5 (curve b). Inset: the bar graph of the oxidation peak currents of Cu^{2+}-Asp/MCH/S1/Au after hybridization with different DNA sequences.

This response was almost identical with that on the non-complementary sequence hybridized electrode (Cu^{2+}-Asp/MCH/S5-S1/Au), suggesting there was no hybrdization reaction between S1 and S5. However, when Cu^{2+}-Asp/MCH/S1/Au was hybridized with the complementary sequences, it was found that the oxidation of the probe electrode showed the largest attenuation, showing that the natural "stem-loop" structure had been converted to the linear double-stranded structure, and therefore the electroactive centers had moved away from the electrode surface, resulting in a small electrochemical signal. The selectivity of the sensor was also investigated by hybridization with the one-base mismatched and the three-base mismatched sequences, and it was found that the DPV signals on both

of the two electrodes were attenuated as compared with Cu^{2+}-Asp/MCH/S1/Au, and the attenuation degree paralleled with the decrease of the mismatching number of the bases. These results showed that the developed biosensor had excellent hybridization selectivity to recognize the complementary, non-complementary and base mismatched sequences. The sensitivity of the DNA biosensor was further investigated by varying the concentrations of the target sequence. As shown in Fig. 7, the peak currents obtained in DPV measurements decreased accordingly with the increasing concentrations of target sequences, showing that more and more perfect DNA duplexes have been formed through the hybridization reaction. The values of the peak currents revealed an excellent correlation with the logarithmic values of C_{S2} ($\lg C_{S2}$) ranging from 1.0×10^{-15}~1.0×10^{-10} M (inset in Fig. 7) with a regression equation of $I_{pa}(10^{-6}$ A)=8.49+0.92lg$(C_{S2}$/M), r=0.952. The detection limit was estimated to be 0.17 fM based on the signal-to-noise characteristic (S/N=3), which is lower than many reported molecule beacon-based biosensors [12, 30, 31], suggesting that the developed biosensors has the higher sensitivity.

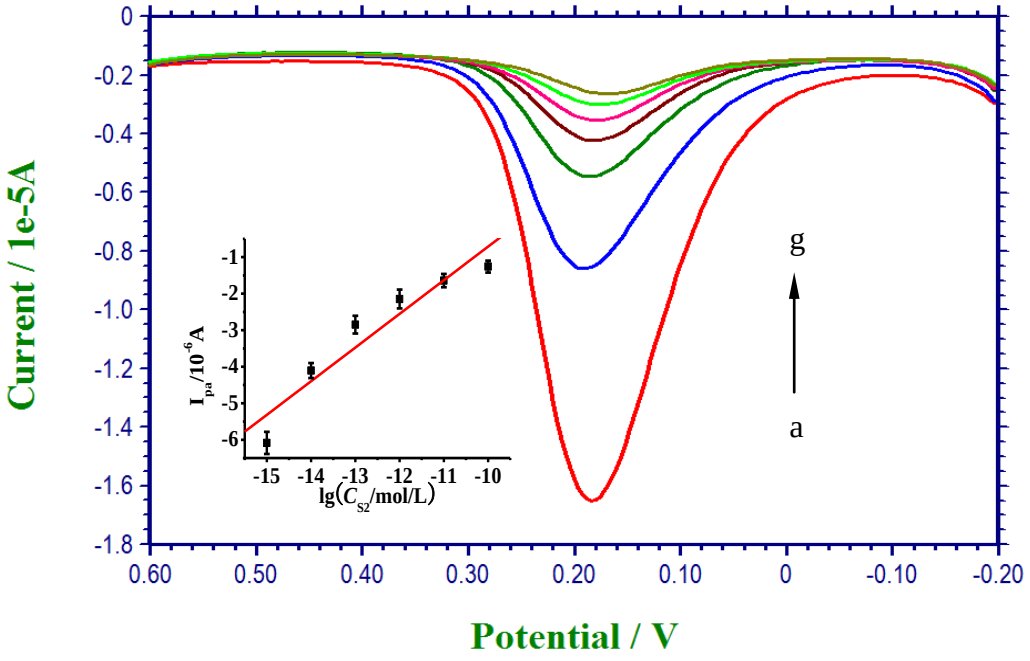

Figure 7. DPVs of Cu^{2+}-Asp/MCH/S1/Au hybridized with various concentrations of the target sequence (a~g: 0, 1.0×10^{-15}, 1.0×10^{-14}, 1.0×10^{-13}, 1.0×10^{-12}, 1.0×10^{-11}, 1.0×10^{-10} M); inset: the linear relationship between I_{pa} and logarithm of S2 concentration($\lg C_{S2}$)

3.5 Reproductivity, regeneration and stability of the biosensor

The reproducibility and regeneration ability of any biosensor is extremely important in practical applications. In our test, five parallel-made DNA biosensors were used to detect 1.0×10^{-10} M target DNA and a relative standard deviation (R.S.D.) of 3.17% (n=5) was obtained, which shows high reproducibility of the DNA electrochemical biosensor. The regeneration ability of this DNA biosensor was also evaluated, which was carried out by dipping the hybridized electrode in 50 mM NaCl at 80 ℃

for 20 min, followed by a rapid cooling in an ice bath for 20 min and subsequently rinsed with DDW, and then the DPV responses of Cu^{2+}-Asp/MCH/S1/Au were recorded. The results showed that the developed biosensor could be repeatedly used for hybridization-denaturation-hybridization circles for 6 times, and only a decrease of 8.5% in DPV response was obtained. Store of Cu^{2+}-Asp/MCH/S1/Au at 4 ℃ for 4 weeks resulted in a change of 2.7% in the initial DPV response, suggesting a good stability of the biosensor.

4. CONCLUSIONS

In summary, a novel electrochemical DNA biosensor based on *in-situ* labeling of *L*-Aspartic acid-copper (Asp-Cu^{2+}) complex on the free terminal of molecule beacon DNA probe is developed for the simple, rapid, specific detection of a target DNA sequence. Our strategy made use of copper complex (Asp-Cu^{2+}) as a signal source. Due to high stability of Asp-Cu^{2+} and the unique stem-loop structure of molecule beacon, the fabricated biosensor exhibited a promising prospective. Experimental results showed that the developed biosensor has good stability, reproductivity, regeneration and specificity. When the biosensor was used for detecting complementary target sequence, a wide kinetic linear range (1.0×10^{-15}~1.0×10^{-10} M) and a low detection limit (0.17 fM) were obtained. Moreover, it was successfully used in distinguishing the complementary sequence from the mismatching sequences and non-complementary sequences.

ACKNOWLEDGMENTS
The work is supported by the NSFC (No. 21275127), NCETFJ (No. JA12204), Science and Technology Project of SIQSAQ (No. 2011QK217), Key Research Foundation of Fujian Education Department (No. JA11166) and Innovation Base Foundation for Graduate Students Education of Fujian Province.

References

1. Z.S. Wu, J.H. Jiang, L. Fu, G.L. Shen and R.Q. Yu, *Anal. Biochem*., 353 (2006) 22.
2. S. Tombelli, M. Minunni and M. Mascini, *Biomol. Eng*., 24 (2007) 191.
3. Q.X. Wang, F. Gao, F. Gao, S.X. Li, W. Weng, F.Q. Liu and K. Jiao, *Biosens. Bioelectron*., 32 (2012) 50.
4. D. Li, A. Wieckowska and I. Willner, *Angewandte Chemie*, 120 (2008) 3991.
5. C.L. Bliss, J.N. McMullin and C.J. Backhouse, *Lab Chip*, 7 (2007) 1280.
6. J.H. Watterson, P.A.E. Piunno and U.J. Krull, *Analytica Chimica Acta*, 457 (2002) 29.
7. B. Guo, Y. Yuan, Y.H. Wu, Q.J. Xie and S.Z. Yao, *Anal. Biochem*., 305 (2002) 139.
8. F. Hook, A. Ray, B. Norden and B. Kasemo, *Langmuir* 17 (2001) 8305.
9. S.J. Li, J. Li, K. Wang, C. Wang, J.J. Xu, H.Y. Chen, X.H. Xia and Q. Huo, *nano Lett*., 4 (2010) 6417.
10. H. Chang, Y. Yuan, N. Shi and Y. Guan, *Anal.Chem*., 79 (2007) 5111.
11. Y.S. Li, X.Y. Zhou and D.Y. Ye, *Biochem. Biophys. Res. Commun*., 373 (2008) 457.
12. F. Wei, J.H. Wang, W. Liao, B.G. Zimmermann, D.T. Wong and C.M. Ho, *Nucleic. Acids. Res*., 36 (2008) e65.

13. Y. Xiao, X.G. Qu, K.W. Plaxco and A.J. Heeger, *J. Am. Chem. Soc*., 129 (2007) 11896.
14. Y.Q. He, K. Zeng, A.S. Gurung, M. Baloda, H. Xu, X.B. Zhang and G.D. Liu, *Anal. Chem*., 82 (2010) 7169.
15. M. Minunni, S. Tombelli, M. Mascini, A. Bilia, M.C. Bergonzi and F.F. Vincieri, *Talanta*, 65 (2005) 578.
16. C. Peter, M. Meusel, F. Grawe, A. Katerkamp, K. Cammann and T. Börchers, *Fresenius J. Anal. Chem*., 371 (2001) 120.
17. F. Gao, Q.X. Wang, M.X. Zheng, S.X. Li, G.L. Chen, K. Jiao and F. Gao, *Int. J. Electrochem. Sci*., 6 (2011) 1508.
18. S. Zhang, G.L. Zhou, X.L. Xu, L.L. Cao, G.H. Liang, H. Chen, B.H. Liu and J.L. Kong, *Electrochem. Commun*., 13 (2011) 928.
19. C.H. Fan, K.W. Plaxco and A.J. Heeger, *Proc. Natl. Acad. Sci*. USA, 100 (2003) 9134.
20. D. Kang, X.L. Zuo, R.Q. Yang, F. Xia, K.W. Plaxco and R.J. White, *Anal.Chem*., 89 (2009) 9109.
21. Y.L. Zhang, Y. Wang, H.B. Wang, J.H. Jiang, G.L. Shen, R.Q. Yu and J.H. Li, *Anal. Chem*., 81 (2009) 1982.
22. Y. Liu, N. Tuleouva, E. Ramanculov and A. Revzin, *Aanl.Chem*., 82 (2010) 8131.
23. G.J. Li, X.L. Li, J. Wan and S.S. Zhang, *Biosens. Bioelectron*., 24 (2009) 3281.
24. X.M. Li, H.Q. Ju, C.F. Ding and S.S. Zhang, *Anal. Chim. Acta*., 582 (2007) 158.
25. R.A. Ammar, A. Nafady, M.F. Amin and M.M.A.-M.E.M. Shoukry, *Int. J. Electrochem. Sci.*, 8 (2013) 1501.
26. C.D. Brondino and R. Calvo, *Inorg. Chem*., 36 (1997) 3183.
27. J. Bertran, L.R. Santiago and M. Sodupe, *J. Phys. Chem*. B 103 (1999) 2310.
28. S.C. Zhang, Y.G. Zhu, C. Tu, H.Y. Wei, Z. Yang, L.P. Lin, J. Ding, J.F. Zhang and Z.J. Guo, *J. Inorg. Biochem*., 98 (2004) 2099.
29. H. Zhu, S.X. Zhang, M.X. Li, Y.H. Shao and Z.W. Zhu, *Chem. Comm*., 46 (2010) 2259.
30. R.M. Castro, P.S. Älvarez, M.J.L. Castanon, A.J.M. Ordieres and P.T. Blanco, *Anal.Chem*., 79 (2007) 4050.
31. Y.J. Niu, Y.J. Zhao and A.P. Fan, *Anal. Chem*., 83 (2011) 7500.